Response characteristics of soil moisture to rainfall for a single grass vegetation in the urban area — A case of regional grassland in Yangzhou City

Jinbai Huang[1*], Jiawei Wen[2], Diwen Luo[1], Chaofan Zhu[1]

(College of Hydraulic Science and Engineering of Yangzhou University, Yangzhou, Jiangsu, China, 225009; College of Information Engineering of Yangzhou University, Yangzhou, Jiangsu, China, 225127)

Abstract: A regional grassland with Bermudagrass in Yangzhou City was adopted as the study location. Based on the analysis of the different rainfall events and soil water content data in the same periods, the response characteristics of infiltration to rainfall were revealed in a certain degree. The surface resistance parameters (r_s) are calibrated according to the soil water content at the depths of a range for 0-30 cm and of the root layer (0-10 cm). Penman-Monteith (P-M) equation was adopted to estimated the hourly evapotranspiration (ET) over the Bermudagrass lawn of the soil layers for the depths of 0-30 cm (ET_{30}) and 0-10 cm (ET_{10}), respectively. Applicability of HYDRUS-1D model for simulating soil water content at different depths was validated. The results indicated that the infiltration depth generally varies with the rainfall event grade, and on the whole, the infiltration depth increases with the improvement of amount of rainfall; the response time for the soil water content in root layer is much shorter with the less soil water content in the topsoil (0-5.5 cm); the increase rate of soil water content raised with increasing of rainfall intensity in the state of unsaturation; ET_{10} accounts for about 78% of ET_{30}, which demonstrates the water consumed by ET is mainly provided by the soil water in the root layer. the rationality of the results of different rainfall events and infiltration depth achieved by the analysis of the observed data were verified via numerical simulation using Hydrus-1D.

Keywords: urban; grassland; rainfall; soil water; ET; Hydrus-1D; infiltration

1. Introduction

Land use and land cover change widely occurs during urbanization (Zhang et al., 2020). Accelerated urbanization continues to convert natural lands to impervious surfaces, resulting in serious impacts to the environment, and affecting the growth of urban plants(Song et al., 2015). The process of urbanization alters the hydrological performance of an area (Armson et al., 2013), urbanization brings a range of environmental challenges as a direct result of the biochemical and physical changes to hydrological systems(Fletcher et al., 2013; Zang et al., 2019). Decreases in the water retention function of various artificial disturbed landform units caused by urbanization activities, compared to original landform units, are the main factor that causes urban water and soil loss and the aggravation of urban floods under certain rainfall conditions and specially designed drainage network capabilities(Baek et al., 2015; Shi et al., 2016). Urban grasslands are expanding rapidly along with urbanization, which is expected to increase at unprecedented rates in upcoming decades. Grassland surface represented that compared with the impervious area, grassland was able to effectively delay time to runoff(Liu et al., 2020). The large and increasing area of urban grasslands and their impact on water justify the need for a better understanding (Duan et al., 2013). Grassland is an indispensable part of urban green space ecosystem, plays an important role in improving regional ecological environment, regulating hydrological cycle and reducing loss of soil and water (Livesley et al.; 2010; Xiong et al., 2014; Xu and Cheng 2019; Yang et al., 2020). Soil moisture plays a critical role in land surface-plant-atmosphere interactions, and direct impacts on food security, human health and ecosystem function (Huang and Shao, 2019). Evapotranspiration (ET) is an important hydrological process in the water cycle and plays a key role in the energy budget and water balance of the earth-atmosphere system (Zhang and Shen, 2007; Zhao et al., 2018). It is of great significance to study the change characteristics of soil moisture and ET of grassland vegetation under the background of urbanization to improve the urban ecological environment and enhance the construction level of sponge city. So many studies indicated that rainfall affects the change of soil moisture. Wiekenkamp et al(2016) performed a research on spatial and temporal occurrence of preferential flow in a forested headwater catchment used the preferential flow model and found that rainfall had a great influence on soil moisture. Liu et al (2020) analyzed the variation characteristics of soil moisture parameters in the process of rainfall, and proposed that rainfall amount was the most prominent rainfall feature for controlling soil moisture response. Chen et al

(2020) conducted a research on response of soil moisture to rainfall event in black locust plantations at different stages of restoration in hilly-gully area of the Loess Plateau, China and found that rainfall infiltration mainly occurred in the 0−60 cm soil depth, rainfall infiltration was mainly jointly influenced by rainfall attributes and soil properties (etc). In order to reveal the response characteristics of soil moisture of grassland vegetation to rainfall under the background of urbanization, in the current study, an urban regional grassland was adopted as the study location. Analysis of the infiltration characteristics for the different rainfall events were carried out, ET over grassland in the study area was calculated and evaluated, and the infiltration depth for the different rainfall events was verified via numerical simulation by using HYDRUS-1D. The results of the current study are expected to provide the scientific basis for the further studies on soil moisture of grassland for urbanization and the improvement of urban ecological environment based on the development of grassland.

2. Materials and methods

2.1 General situations of the study area

Yangzhou City is located in the middle of Jiangsu Province, the southern of Jianghuai Plain. The climate belongs to a subtropical humid monsoon. Annual average temperature is 16.1 ºC. Annual average rainfall is about 1000 mm while 67% of the total is concentrated in main rainy season from May to September(Zhou et al., 2019). Yangzhou is one of the national ecological garden cites of China. There are many green spaces and parks in the urban area, with the green coverage rate of 44.03%, which plays an important role in improving water circulation and reducing waterlogging in Yangzhou urban area.

A regional artificial lawn in Yangzijin Campus of Yangzhou University was chosen as the study area, which is located in the southwest of Yangzhou City (Geographical coordinates of a control point: 32 ° 20'58 " N, 119 ° 23'51" E; area: 340m^2). The study area is covered with a single species of grass-Bermudagrass, and the coverage is nearly 100% (Fig. 1). Bermudagrass is a perennial warm season herb with the main growth period from May to September. It has the characteristics of drought resistance, weed resistance and strong adaptability, with root depth of 8-10 cm. As a main green grass, Bermudagrass has been widely planted in parks, communities and schools in southern

China.

According to the field survey, the 0-60 cm soil in the study area is mainly silty loam, the groundwater (phreatic water) level varies with seasons, about 2-5m from the ground. There are many buildings and impervious pavement around the study area.

(a) (b)

Fig. 1 Grass cover (partial view) and field observations at the study area

2.2 Data acquisition

An automatic weather station (mode: U30-nrc-10-s100-000; Onset Company, USA) was set up in the study area to record hourly temperature, rainfall, solar radiation, wind speed, and relative humidity. The observation point elevation is 14 m, and the equipment height is 2 m (Fig. 1b). Soil water contents were observed by using soil moisture meters (mode: H21-002; Onset Company, USA) on two sites, the observation depth on one point (P1) is 10 cm, 25 cm and 40cm, while on another point (P2) is 5 cm, 15 cm, 30 cm and 60 cm, respectively.

To evaluate the response characteristics of soil moisture in root layer of Bermudagrass lawn to different rainfall processes, soil simple experiment was carried out according to the weather forecast information. The topsoil (0～5.5cm) of the soil water content on P1 was sampled and weighed before each rainfall, and then weighed after drying to determine the initial water content of the topsoil soil. Meanwhile, a tipping bucket rain gauge (mode: 7852M-L10, Onset Company, USA) was used to measured rainfall by an interval of 10 min, while soil water content on P1 (10, 30, and 60cm) was measured every 10 min during the periods of 10min rainfall observation.

Additionally, the soil samples at different depths in the study area were collected. Laser particle

size analyzer (model: Mastersizer 3000E; Malvern Copmpany, UK) was used to measure the particle composition of soil samples, and the particle size distribution (percentage content of clay, sand and silt) was obtained.

2.3 ET calculation

Penman-Monteith（P-M）equation (E.q 1) is adopted to calculate ET over grassland in the study area, as it is widely used in the calculation of ET over various vegetation (Longobardi and Villani 2013; Hadi and Farah 2018; Djaman et al., 2019).

$$ET = \frac{\Delta(R_n - G) + c_p \rho \frac{(e_s - e_a)}{r_a}}{l[\Delta + \gamma(1 + \frac{r_s}{r_a})]} \quad (1)$$

where, l is the latent heat of vaporization (MJ·kg^{-1}); c_p is the specific heat of air at constant pressure (1.0×10^{-3} MJ·kg^{-1}·K^{-1}); Δ is a slope of the saturation vapor-pressure at air temperature (kPa·K^{-1}); R_n is the net radiation (MJ·m^{-2}·h^{-1}); G is the soil heat flux (MJ·m^{-2}·h^{-1}); ρ is the air density at constant pressure (kg·m^{-3}); γ is the psychometric constant (kPa·K^{-1}); e_s is the saturated vapor-pressure at air temperature (kPa); e_a is the actual vapor-pressure (kPa); r_a and r_s represent the aerodynamic resistance and the surface resistance, respectively, (s·m^{-1}).

The calculation methods of each factor in equation (1) was introduced in Zhou et al (2019). The surface resistance (r_s), which controlled by soil water content for the soil layer depth of 0-30cm (r_{s30}) and for the root layer (depth about 10cm) was calibrated, respectively, according to Kumura et al (2005) and Zhou et al (2019), the results were determined by equation (2) and equation (3), respectively.

$$r_{s30} = 26\,498\exp(-4.784\theta_{30}) \quad (2)$$

$$r_{s10} = 21\,980\exp(-1.258\theta_{10}) \quad (3)$$

where, θ_{30} is the average soil water content in the soil layer of 0-30cm (cm^3·cm^{-3}); θ_{10} is the soil water content for the depth of 10cm (cm^3·cm^{-3}).

2.4 Hydrus-1D model development

2.4.1 Basic equations

Simulations of soil water content at different depths were performed with Hydrus-1D model to validate the infiltrated depth for the different rainfall events. Richards' equation was used in Hydrus-1D numerically solves the soil moisture movement in variably saturated porous media (Narjary et al., 2020; Fairouz et al., 2020). Richards' equation (E.q 4) with water content as the dependent variable is used to construct the water transport model.

$$\begin{cases} \dfrac{\partial\theta}{\partial t}=\dfrac{\partial}{\partial z}\left[D(\theta)\dfrac{\partial\theta}{\partial z}\right]+\dfrac{\partial K(\theta)}{\partial z}-S \\ K(\theta)=K_S\theta_e^{l}\left[1-(1-\theta_e^{\frac{1}{m}})^{m}\right]^2 \\ \theta_e=\dfrac{\theta-\theta_r}{\theta_s-\theta_r}=\left[1+(\alpha|h|)^{n}\right]^{-m},\ m=1-\dfrac{1}{n},(0<m<1,\ n>1) \end{cases} \tag{4}$$

where, θ represents the soil water content ($cm^3 \cdot cm^{-3}$); t is time factor (h); z is the vertical distance from the ground (soil depth), the coordinate is positive downward (cm); $D(\theta)$ is the soil water diffusivity ($cm^2 \cdot h^{-1}$); $K(\theta)$ is the unsaturated hydraulic conductivity ($cm \cdot h^{-1}$); S is the source (or sink) of soil water, which represents the water absorption rate of crop root ($cm \cdot h^{-1}$); K_s is the saturated hydraulic conductivity ($cm \cdot h^{-1}$); θ_e, θ_s, and θ_r are the effective, saturated and residual water content ($cm^3 \cdot cm^{-3}$); α and n represent the empirical shape parameters, m = l-1/n; l is a pore connectivity parameter; h is soil matrix potential (cm).

2.4.2 Definite solution conditions

The initial condition is the observed value of soil water content at the beginning of calculation. The upper boundary condition is set as the atmospheric boundary condition with surface layer which includes hourly (1h series) rainfall and potential evapotranspiration (ET_0). Hourly ET_0 was estimated by Penman-Monteith model which recommended by FAO 56 (Allen et al., 1998). The lower boundary is located in the unsaturated zone because it does not reach the phreatic layer, so it is set as the free drainage boundary. The definite solution conditions are represented as equation (5).

$$\begin{cases} \theta(z,t)=\theta_0(z), t=0 \\ \left[-D(\theta)\dfrac{\partial h}{\partial z}+K(\theta)\right]_{z=0}=q_0(t), t>0 \\ \theta(L,t)=\theta_L(t), t>0 \end{cases} \quad (5)$$

where, θ_0 is initial soil water content ($cm^3 \cdot cm^{-3}$); q_0 (t) is soil water flux ($cm \cdot d^{-1}$); L is the vertical depth of the lower boundary (cm); $\theta_L(t)$ is soil water content at the lower boundary ($cm^3 \cdot cm^{-3}$).

2.4.3 Parameter calibration

According to the screening results of soil particle size achieved by the experiments of particle composition of soil samples (Table 1), Rosetta module based on neural network is used to preliminarily determine the parameters of saturated water content θ_s, residual water content θ_r and saturated hydraulic conductivity K_s (etc)(Li et al., 2015). On this basis, comparisons between the Hydrus-1D calculated results and the measured soil water contents at various depths (5, 15, 30, 60cm) were performed. Adjustment of each parameter values and repeated model calculation were carried out to reduce the difference between the simulated results and the measured one, so as to achieve the calibration of parameters (Table 1).

Table 1 The measured data of soil physical properties and main parameters obtained by combined using Rosetta and model calculation

Soil depth	Sand grain % 50~2000μm	Silt % 2~50μm	Clay % <2μm	θ_s cm^3/cm^3	θ_r cm^3/cm^3	α cm^{-1}	n	K_s cm/min	l
0~10cm	27.10	65.71	7.19	0.35	0.045	0.0047	1.23	2.08	0.5
10~20cm	21.78	69.76	8.48	0.37	0.051	0.0046	1.23	2.33	0.5
20~40cm	17.72	74.05	8.24	0.36	0.056	0.0048	1.33	1.85	0.5
40~60cm	19.33	71.23	9.45	0.37	0.053	0.0045	1.42	1.43	0.5

3. Results and discussion

3.1 Response time of soil moisture in root zone to rainfall

Six periods with rainfall events during April to June in 2019 were chosen to analyze the changes of soil water content for different rainfall processes, and to estimate the response time of soil moisture in root layer to rainfall. The response time of soil moisture in root layer refers to the time from the beginning of rainfall to the beginning of soil water content change at the depth of 10 cm. The soil water content in topsoil (5.5cm) and response time of the soil depth of 10 cm for each rainfall event are shown in Table 2.

Table 2 Response times of the soil water content to the different rainfall events in the grass root zone at the depth of 10cm

No.	Soil water content before rainfall/$cm^3 \cdot cm^{-3}$		Response time / min
	Topsoil / 5.5cm)	Root zone /10cm	
1	0.215	0.322	$620<t\leqslant630$
2	0.021	0.201	$t\leqslant10$
3	0.023	0.195	$t\leqslant10$
4	0.045	0.254	$t\leqslant10$
5	0.187	0.329	$50<t\leqslant60$
6	0.131	0.310	$30<t\leqslant40$

Note: the response time is expressed by a time interval of 10 minutes as the unit time of rainfall and soil water content is set to 10 min.

The temporal process of each rainfall event and the change of soil water content at different depths are shown in Figure 2. In a period from April 28th 13:00 to April 30th 13:00, amount of rainfall is 6.4 mm with the maximum intensity of 0.42 $mm \cdot min^{-1}$. The response time is more than 10 h due to the frequent rainfall interruption, the short durations and small amount of periodic rainfall(Fig. 2a). Meanwhile, As Bermudagrass lawn with high coverage and dense, vegetation interception and ET consume most of the rainfall, and there is no effective infiltration within a few hours after the rainfall. After the soil water content at depth of 10cm (root layer) reached the peak, the soil water content at depth of 25 cm increased slowly, while the soil water content at depth of 40 cm remained relatively stable (Fig. 2a).

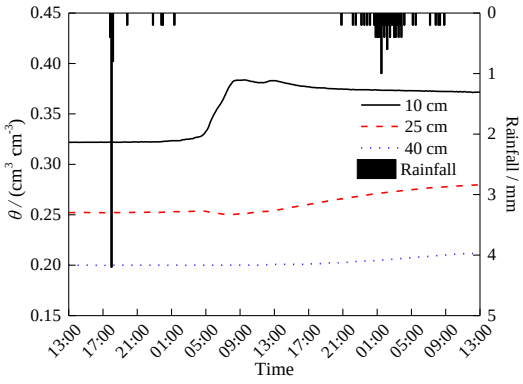

184

185 (a) 04.28 13:00 ~ 04.30 13:00

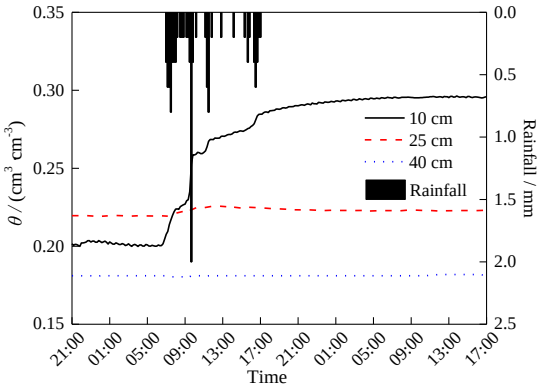

(b) 05.25 21:00 ~ 05.27 17:00

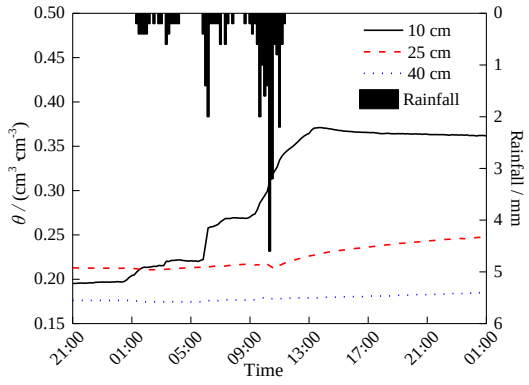

186

187 (c) 06.05 21:00 ~ 06.07 1:00

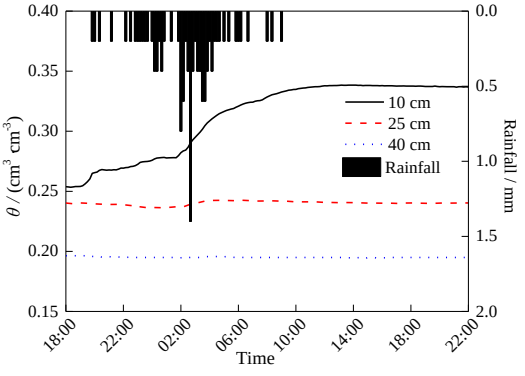

(d) 06.17 18:00 ~ 06.18 22:00

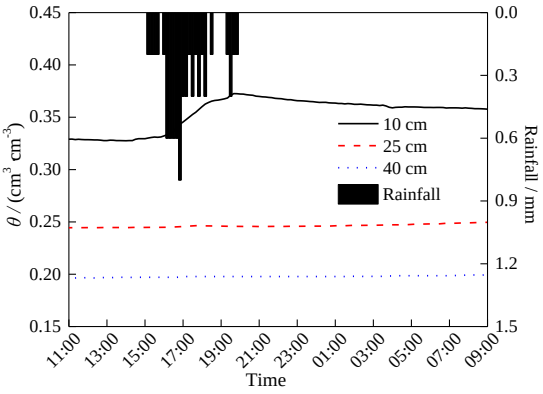

188

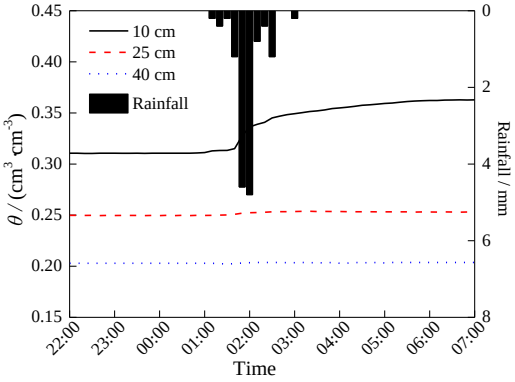

189

(e) 06.20 11:00 ~ 06.21 9:00 (f) 06.28 22:00 ~ 06.29 7:00

Fig. 2 Changes of the soil water content under the different rainfall events

The change processes of the soil water content at the depths of 10, 25 and 40 cm in a period from May 25th 21:00 to May 27th 17:00 were depicted in Figure 2b. A relatively concentrated rainfall event occurred on May 26th with the rainfall amount of 12.6 mm and the maximum intensity of 0.20 mm·min^{-1}; the response time of root layer to rainfall within10 min, and the increase range of soil water content in root layer is significantly affected by rainfall intensity; while the soil water content at 25 cm and 40 cm remained stable. The main reasons are that the original soil water content in topsoil was low before the beginning of rainfall (Table 2), and the soil water content in root zone did not attain saturation after the end of rainfall, and the soil water content below 25 cm had not gotten recharged from infiltration.

Figure 2c shows that a rainfall event occurred from June 5th 22:00 to June 6th 11:00 with rainfall mount of 30.4 mm and the maximum intensity of 0.46 mm·min^{-1}; the water content in topsoil was low before rainfall, and the response time to rainfall was less than 10 min; the soil water content in root zone increased slowly when the rainfall intensity is small and the increase rate improved with the increasing of rainfall intensity. Soil water content in root zone increased significantly during the 5:50-6:20 and 9:10-11:20 on June 6th as the maximum rainfall intensity reached 0.20 and 0.46 mm·10 min^{-1} in these two periods, respectively, which indicates that rainfall intensity greatly impacts on the change of soil water content in root zone. The soil water content at 25 cm began to rise slowly from the time of the maximum rainfall intensity, while the soil water content at 40 cm remained stable.

Figure 2d represents the temporal change process of the soil water content at the depths of 10, 25 and 40 cm from June 17th 18:00 to June 18th 22:00 and a rainfall event occurred in a period from June 17th 20:00 to June 18th 9:00 with the rainfall amount of 14 mm and the maximum intensity of 0.14 mm·min^{-1}; the response time of water content at the depth of 10 cm to rainfall is within 10 min, and the soil water content at 25 cm increased slightly when the rainfall intensity reached the maximum, while the soil water content at 40 cm remained stable.

A relatively concentrated rainfall event occurred on June 20th (14:00 to 20:00) with the rainfall

amount of 8 mm and the maximum intensity of 0.08 mm·min^{-1}; The response time of water content at 10 cm to rainfall is 50-60 min, the soil water content at 25 and 40 cm remained stable during the process of this rainfall (Fig. 2e).

Figure 2f represents the temporal change process of the soil water content at the depths of 10, 25 and 40 cm from June 17th 18:00 to June 18th 22:00 and a rainfall event occurred in a period from June 28th 22:00 to June 29th 7:00 with the rainfall amount of 14 mm and the maximum intensity of 0.48 mm·min^{-1}; the rainfall duration is relatively short and the intensity is comparative large; the response time of water content at 10 cm to rainfall is 30-40 min. The main reasons are that the initial soil water content in topsoil and root zone were relatively higher before rainfall (Table 2), which resulted in the infiltration rate decreased.

Sum up the above analysis, the response time of soil water content in root zone to rainfall is affected by the actual rainfall process and underlying surface conditions. Generally, with the increase of rainfall intensity, the response time of soil water content in root zone to rainfall is shorter. Under the condition of the little difference of rainfall intensity, the lower the initial water content in topsoil causes the shorter response time of root layer to rainfall, and the faster infiltration rate of topsoil. The main reason is that the smaller water content of the soil results in the lower soil water potential, and the suction of water increased, the infiltration rate improves. From beginning of rainfall to a short time span after the end of rainfall, the water content below 25 cm can not or can only get a small amount of effective infiltration recharge, while the soil water content at 40 cm remained relatively stable, which indicates that the grassland vegetation in the study area has a strong interception function. Before the soil water content in root zone reaches saturation, soil water content is significantly impacted by rainfall intensity, the bigger rainfall intensity causes the faster increasing rate of soil water content. Yang et al. (2008) obtained the similar results in an another research conducted on the Loess Plateau, China. However, due to the limitation of observed data, quantitatively evaluation for the relationship between the change of rainfall intensity and the increment of soil water content in root zone have not performed in the current research.

3.2 ET

Hourly ET of the soil layer for the depth of 0-30cm (ET_{30}) and of the root zone (ET_{10}) were estimated

by using the calibrated surface resistances of r_{s30} and r_{s10}, respectively. The estimated period is from July 2018 to June 2019, which included the main growth period of grass, and the results can represent the change process of ET over grassland (Bermudagrass lawn). ET30 and ET10 are shown in Figure 3. The maximum ET_{10} and ET_{30} are 1.04 and 1.11 mm, respectively, ET_{30} is higher than that of ET_{10} at the corresponding time. Whereas, the temporal change processes of ET_{10} and ET_{30} are similar, and the correlation coefficient is 0.99. Seasonal ET changes obviously, ET exhibits comparatively high values in the main growth period of grass from June to September, while exhibits relatively low levels in non-main growth period (January, February, December, etc). Accumulated values of ET_{30} and ET_{10} are 396 and 309 mm, respectively, which accounted 39.6% and 30.9 % of the rainfall in the same period. Accumulated value of ET_{10} is 78% of that of ET_{30}, which indicates that soil water in the root zone provides the main part of the consumed water by ET.

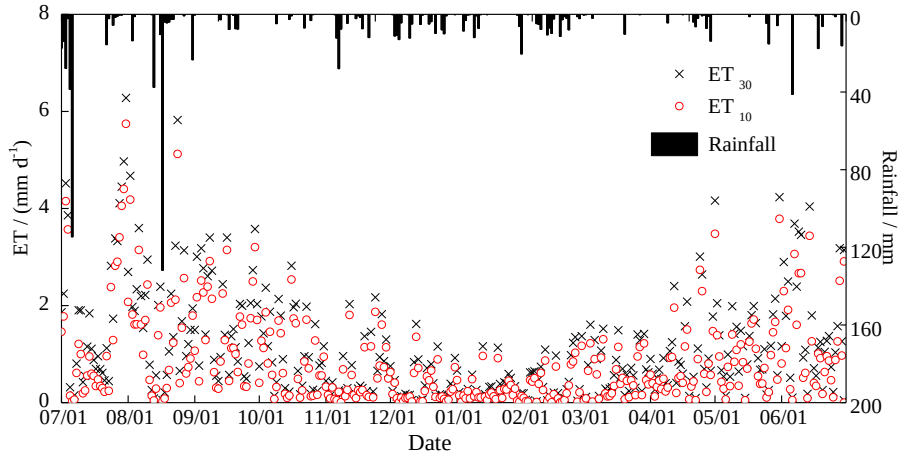

Fig. 3 Calculated results of hourly ET_{30} and ET_{10}

Figure 4 shows the randomly selected results of hourly ET_{10} on 4 non-rainfall days in different seasons. The maximum difference of ET_{10} between two adjacent hours is 0.10 mm on October 1st 2018, and daily ET_{10} is 0.41mm. on December 30th 2018, ET_{10} did not show obvious fluctuation and its maximum difference between two adjacent hours is 0.03 mm, and daily accumulated value is 0.28 cm. On April 7th 2019, ET_{10} exhibited fluctuations in different ranges, the maximum difference value between two adjacent hours is 0.09 mm, and the daily accumulated vale was 0.49 mm. ET_{10} fluctuated frequently on June 30th 2019, the maximum difference value between two adjacent hours was 0.37 mm, and daily accumulated value was 2.91mm. Daily ET_{10} generally increases from a certain time in the morning, then decreases gradually after reaching the peak, and

approaches to 0 after a certain time in the evening. When the meteorological factors (such as temperature and solar radiation), which significantly affect ET_{10}, change obviously in a certain period of daytime, ET_{10} shows a fluctuating upward or downward trend. During the main growth period from June to September, soil water content and the main meteorological factors, which significantly affect ET, mostly maintain annual comparative high levels cause the relatively big value of accumulated daily ET_{10}. Daily change of ET_{10} in winter is smaller than that in other seasons.

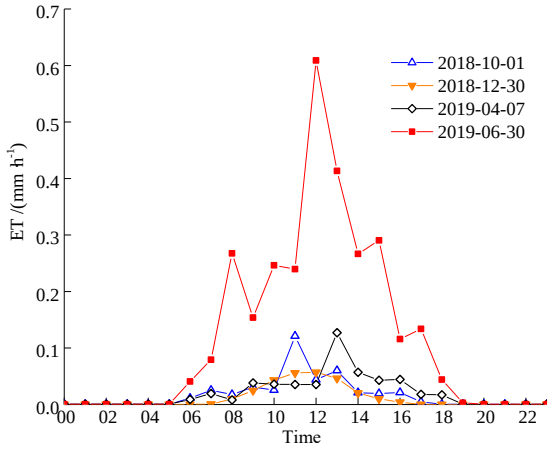

Fig. 4 Daily change of ET_{10}

3.3 Amount of rainfall and infiltration depth

The 8 rainfall events and the observed soil water content on P2 (at depths of 5, 15, 30 and 60 cm) in the same periods were chosen for the analysis to explore the relationship between amount of rainfall and infiltration depth. The grades of 8 rainfall events are classified (Table 3), according to the classification standard of China Meteorological Administration.

The maximum duration of the selected rainfall event is 23h. In order to ensure the sufficient infiltration for each rainfall event, the periodic time of 4 day was adopted for analyzing each rainfall event and infiltration. The amount of rainfall and the infiltration depth of each period are shown in Table 3, the change of soil water content at different depths is shown in Figure 5.

Table 3 Index of the 8 rainfall events and infiltration depth

Grade of rainfall event	The periodic time	Rainfall concentrated time	Rainfall amount /mm	Infiltration depth / cm

Light rain	2018.10.08～10.11	10.09 14:00～16:00	4.8	<5
	2018.05.30～06.02	05.30 22:00～05.31 7:00	8.9	5～15
Moderate rain	2018.07.21～07.24	07.22 11:00～07.23 3:00	17.8	15～30
	2018.04.04～04.07	04.05 12:00～23:00	24.0	
Heavy rain	2018.08.12～08.15	08.13 00:00～17:00	37.6	30～60
	2019.06.05～06.08	06.06 1:00～14:00	41.2	>60
Rain storm	2019.08.09～08.12	08.10 2:00～08.11 1:00	55.0	>60
	2018.05.23～05.26	05.24 22:00～5.25 20:00	107.0	>60

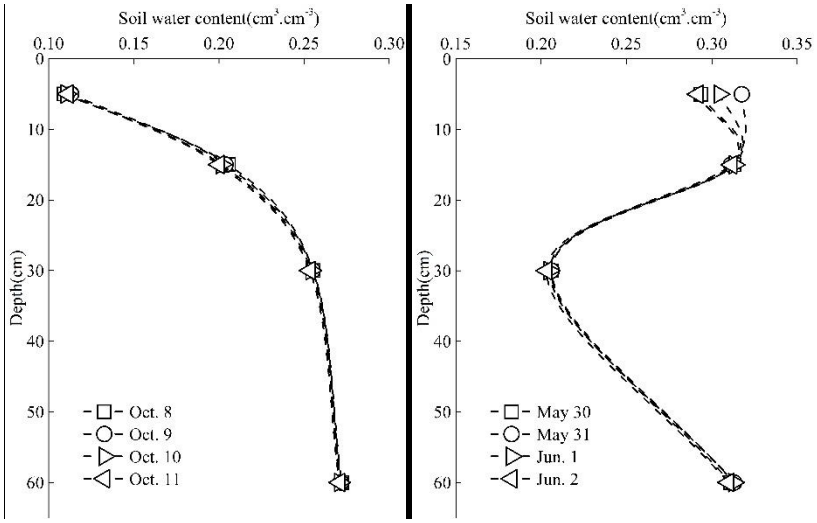

（a） （b）

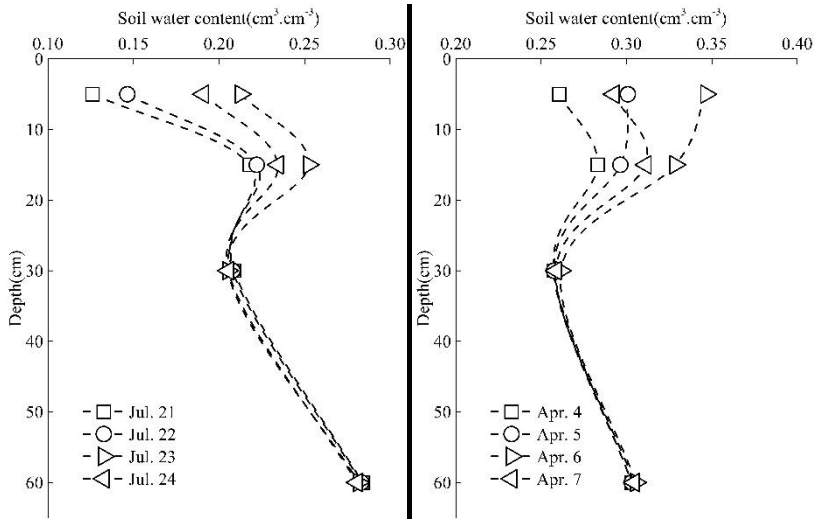

289 （c） （d）

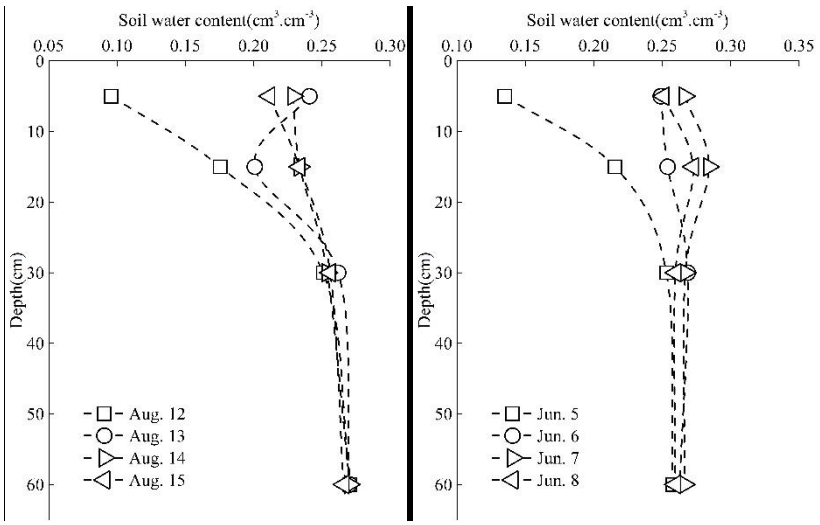

290

291 （e） （f）

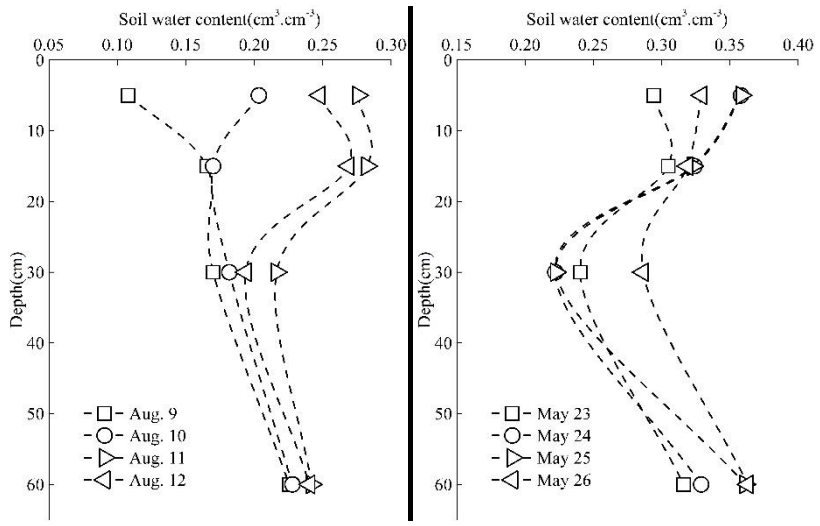

292

293 （g） （h）

294 Fig. 5 The change of soil water content at the depths of 5, 15, 30 and 60 cm during the selected 8 periods

295 Figure 5a shows the changes of soil water content at the 4 depths (5, 15 30 and 60 cm) during
296 the period from October 8th to October 11th in 2018. Rainfall mainly concentrated on October 9th,
297 and amount of rainfall was 4.8 mm (Table 3). Soil water content at the 4 depths remained stable,
298 that is, the rainwater infiltration did not reach the depth of 5cm. The main reason is that the
299 Bermudagrass lawn vegetation has a strong interception function that effective infiltration of this
300 rainfall event did not occur. A relatively concentrated rainfall event occurred in a period from 22:00
301 on May 30th to 7:00 on May 31st with rainfall amount of 8.9 mm. Soil water content at the depth of

5 cm increased obviously due to rainwater infiltration, while soil water content of 15, 30 and 60 cm remained stable during the 4 days (2018.05.30-06.02). The above two rainfall events belong to light rain, the amount of rainfall of the second rainfall event (8.9mm) is more than that of the previous one (4.8mm), and its infiltration depth is also greater than that of the previous one.

Two moderate rains happened on July 22nd to July 23rd and April 5th 2018 and amount of the two rainfall events were 17.8, 24.0 mm, respectively. Soil water content at 5 and 15 cm rose obviously due infiltration cause by the two rainfall events, whereas soil water content at 30 and 60 cm remained stable, that is, the infiltration depth was less than 30 cm (Fig. 2c, Fig. 2d).

Two heavy rainfall events occurred on August 13th 2018 and June 6th 2019 with amount of rainfall of 37.6 and 41.2 mm, respectively. Soil water content of 5, 15 and 30 cm increased in different degree due to infiltration; soil water content at 60 cm remained relatively stable during the rainfall occurrence and after the end of rainfall on August 13th, 2018, which indicated that rainfall infiltration did not reach 60 cm (Fig. 2e). Due to infiltration effect of the rainfall event on June 6th, 2019, soil water content of 60cm increased slightly (Fig. 2f), that is, the infiltration of this rainfall event reached 60cm.

Two rainstorms occurred on May 24th to 25th 2018 and August 10th to 11th 2019 with rainfall amount of 107 and 55 cm, respectively. Soil water content at 5, 15, 30 and 60 cm visibly increased and the infiltration depth exceeded 60 cm.

The analysis results of randomly selected rainfall events (including but not limited to the above 8 rainfalls) and the change of soil water content in the same period indicated that the infiltration depth generally varies with different amount of rainfalls. The more amount of rainfall generally resulted in the greater infiltration depth. To the study area (Bermudagrass lawn), the infiltration depth of light rain is generally less than 15cm, and that of moderate rain is mostly less than 30cm; while the infiltration depth of heavy rain is generally more than 30cm (partial more than 60cm), and the infiltration depth of rainstorm is even greater (> 60 cm). Such results are basically consistent with those of Wu et al. (2018), which achieved by a similar research.

3.4 Validation of Hydrus-1D

Root mean square error (*RMSE*, E.q (6)) and Nash efficiency coefficient (*NSE*, E.q (7)) were

combined used to evaluating the simulation error of Hydrus-1D. *RMSE* represents the average error between the simulated result and the measured one, its value is much closer to 0，the error is smaller, and the simulated results is much accurate. *NSE* characterizes the model efficiency, the model is more reliable in case of its value is much closer to 1.

$$RMSE = \sqrt{\frac{1}{n}\sum_{i=1}^{n}\left(S_i - O_i\right)^2} \tag{6}$$

$$NSE = 1 - \frac{\sum_{i=1}^{n}\left(O_i - S_i\right)^2}{\sum_{i=1}^{n}\left(O_i - \overline{O_i}\right)^2} \tag{7}$$

where, S_i and O_i represent the simulated value and the measured one; $\overline{O_i}$ is average value of the measured results.

Hourly series simulation of soil water content at the depths of 5, 15, 30 and 60 cm in a period from April 4th 2018 to September 19th 2019 (total 1281h) was carried out by using Hydrus-1D, the results are shown in Figure 6. Figure 6 depicts that the simulated results of soil water content at different depths appropriately reproduce the change process of the measured results. However, slight differences exist in the simulated results of soil water content at different depths. The difference between the simulated result and the measured value for the depth of 5cm is periodically larger than those of other 3 depths (Fig. 6). *RMSE* of the simulated result of 5 cm is the maximum (0.034 $cm^3 \cdot cm^{-3}$) while *NSE* is the minimum (0.77) among the errors of the 4 depths (Table 4), which indicates the simulation error of the 5 cm is the maximum. With the increase of depth, the simulation accuracy increases (Table 4). Soil water content of 5cm is significantly affected by rainfall infiltration and ET, and the function of Hydrus-1D for soil water simulation is limited to the vertical movement, and without calculation function of the horizontal diffusion. In the process of vertical calculation of soil water, vegetation interception is regarded as partial ET_0, which can not be accurately estimated in the rainfall process (Sutanto et al., 2012). Because the root depth of Bermudagrass is about 10 cm, with the increase of depth, the effect of ET and rainwater infiltration on soil water content gradually decreases, and the accuracy of simulation results gradually increases. Although the simulation error of 5cm is the maximum among those of the 4 depths, however, the

simulated results are still with comparatively higher accuracy as *NSE* is approximately 0.80. The results of error evaluation exhibit that Hydrus-1D is applicable to the simulation of soil water content in the study area, and the simulation results have relatively high accuracy.

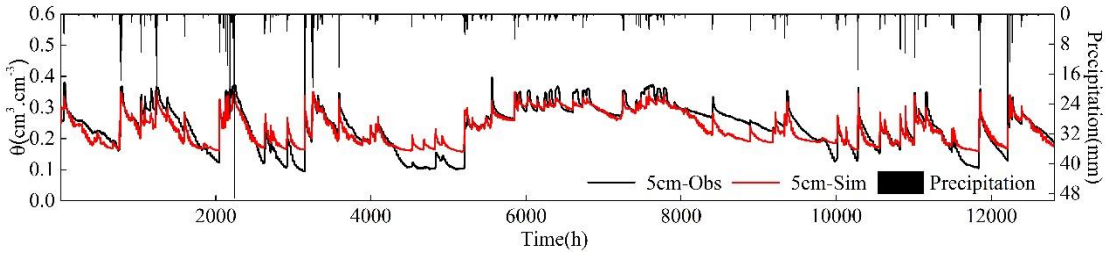

（a）5cm

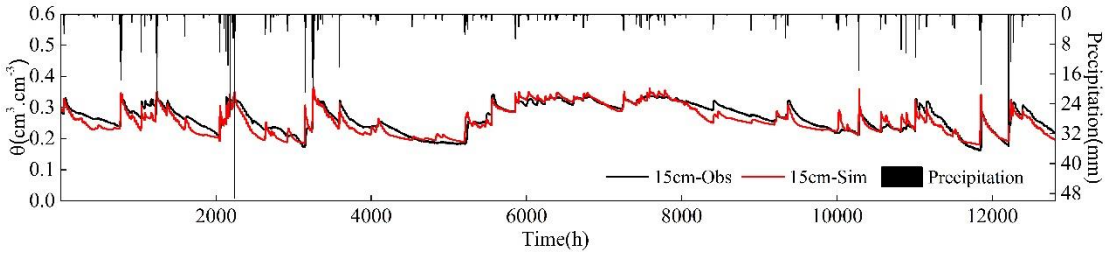

（b）15cm

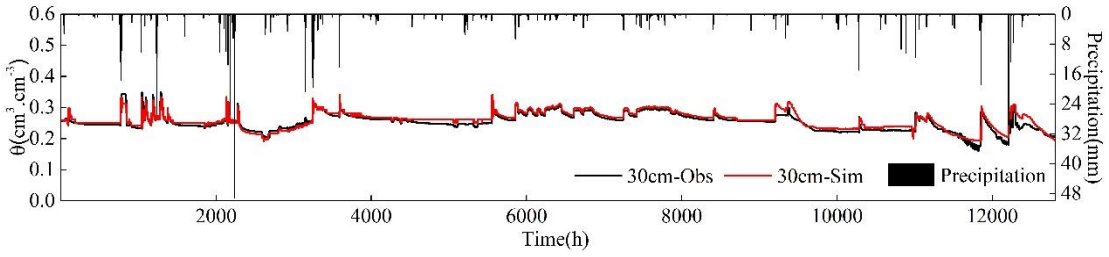

（c）30cm

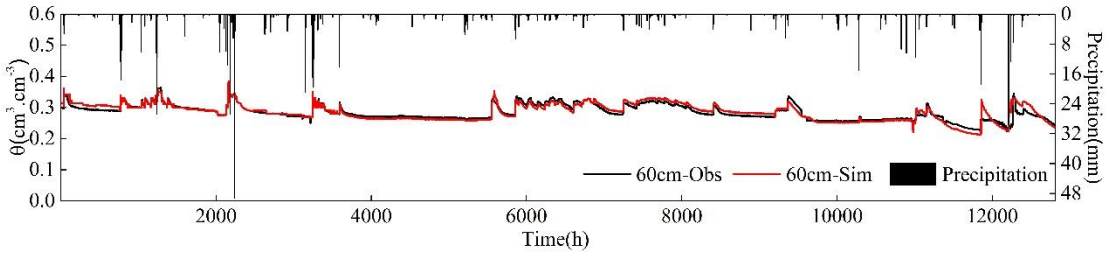

（d）60cm

Fig. 6 The simulated results of soil water content for 4 measured depths of the study area

（Sim: simulated result; Obs: observed value）

Table 4 Index of the simulation errors

Depth	5 cm	15 cm	30 cm	60 cm
RMSE	0.034	0.022	0.015	0.012
NSE	0.77	0.78	0.83	0.84

3.4 Model validation of infiltration depth

To verify the rationality of the results on the relationship between rainfall amount and infiltration depth for different rainfall events based on the analysis of observation data (Fig. 5), the observed results of 8 rainfall events (Table 2), the measured and simulated results of soil water content at different depths in corresponding time of each rainfall concentrated period were extracted and processed as shown in Figure 7.

Figure 7a depicts that during the light rain event on October 9, 2018, and before and after it, the measured results of soil water content of 5cm remained stable, while the simulated results slightly increased during the rainfall concentrated period. In the process of Hydrus-1D calculation, rainfall caused water input at the model upper boundary and soil water content in the model increased, which resulted in slight difference between the measured results and simulated one of soil water content at depth of 5 cm. It thereby confirms that the Bermudagrass in the study area has a strong interception effect. Figure 7b shows the change of soil water content during another light rainfall event happened on May 30th to 31st in 2018, and before and after it. The measured value and the simulated one of soil water content at 5 cm increased in a similar increment, whereas, the measured and simulated results of soil water content at 15 cm remained stable, by which the rationality of the relationship between amount of rainfall and infiltration depth for light rain (Fig. 5b) is verified.

The simulated results of soil water content for the two moderate rainfall events (Table 3) show

that soil water content at depth of 30 cm did not change, while obviously increased at the depth of 15 cm (Fig. 7c, Fig. 7d). The simulated results are consistent with the analyzed results of relationship between moderate rainfall and the infiltration depth (Table 3).

The simulated results of soil water content for heavy rain show that infiltration depth was less 60 cm for a heavy rainfall occurred on August 13th 2018 (Fig. 7e), while infiltration depth reached 60 cm caused by another heavy rain on June 6th 2019 (Fig. 7f). These results validate the relationship between heavy rain and the corresponding infiltration depth (Table 3).

The simulated results of soil water content for the two rainstorms (Table 3) represent that soil water content at different depths increased visibly (Fig. 7g, Fig. 7h), and the downward water release occurred at the lower boundary (soil water flux is not 0 at depth of 60 cm) in the process of model calculation, which indicates infiltration depth exceeded 60 cm. The rationality of infiltration depth caused by rainstorm, which is thus verified.

According to the above analysis, Hydrus-1D can be used to accurately estimated the infiltration depth for different rainfall events in case of absence of measured soil water content for the study area.

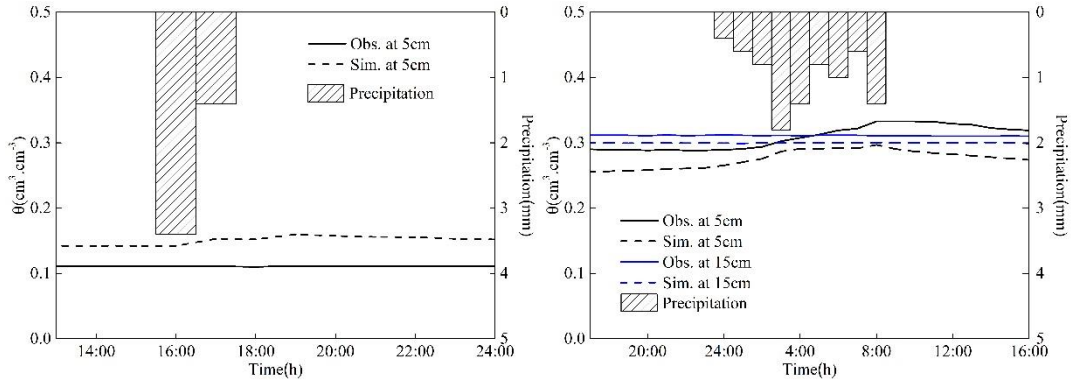

（a）2018/10/9 12:00～24:00　　（b）2018/5/30 17:00～5/31 16:00

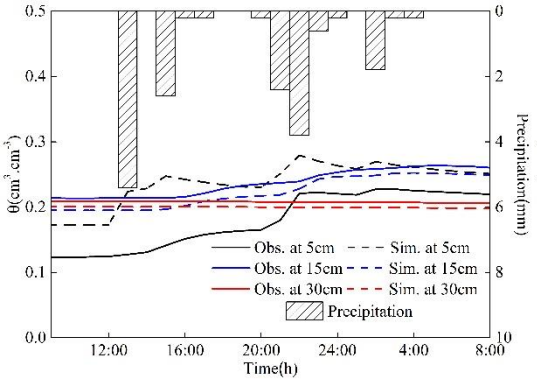

410

411 （c）2018/7/22 17:00～7/23 8:00

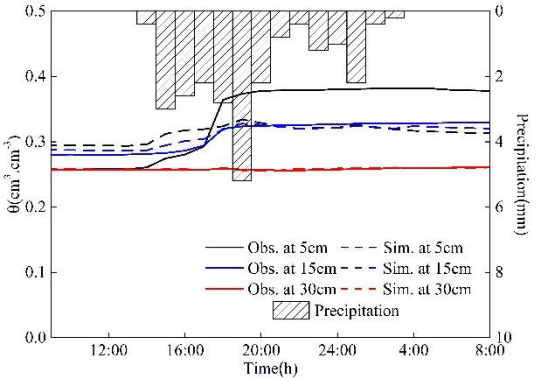

（d）2018/4/5 8:00～4/6 7:00

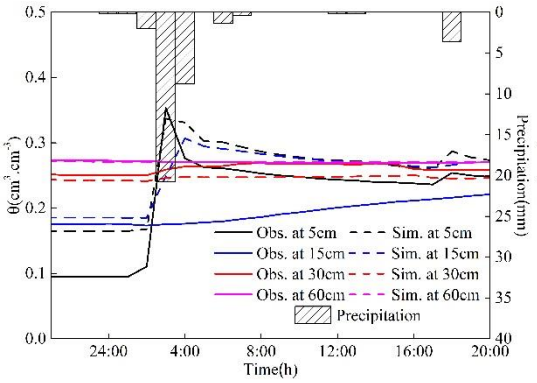

412

413 （e）2018/8/12 21:00～8/13 20:00

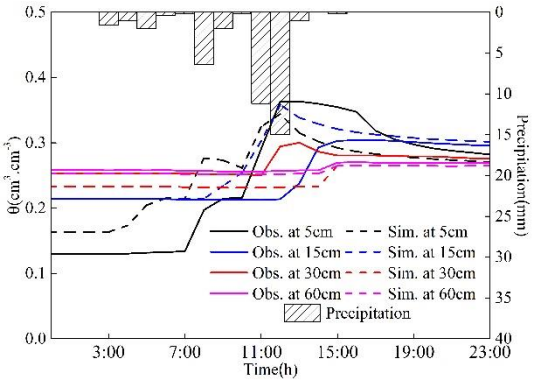

（f）2019/6/6 00:00～23:00

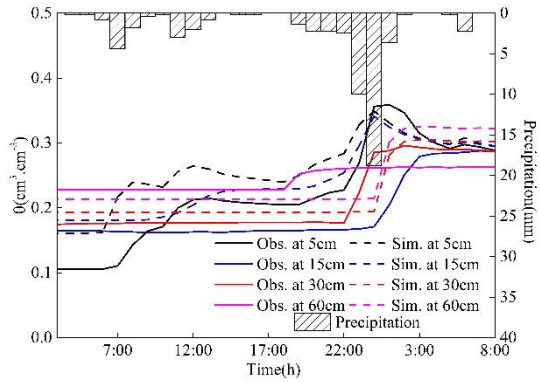

414

415 （g）2019/8/10 3:00～8/11 8:00

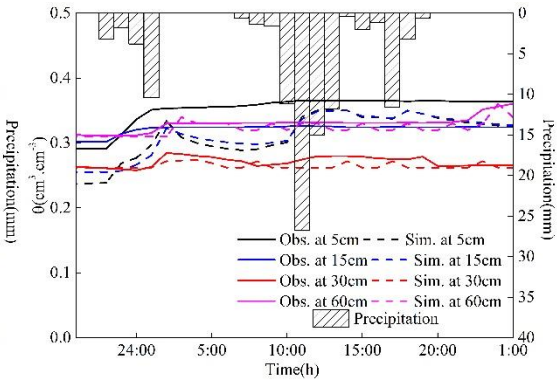

（h）2018/5/24 20:00～5/25 1:00

416 **Fig. 7 The change processes of soil water content at the 4 measured depths for 8 rainfall events**

417 **（Sim: simulated result; Obs: observed value）**

418 # 4. Conclusions

419 In the current research, a regional urban grassland with a single type of grass (Bermudagrass) was

420 chosen as the study location, the response characteristics of soil water to rainfall such as the

relationship between rainfall intensity and response time of soil moisture in root zone, the relationship between amount of rainfall and infiltration depth, and daily ET change characteristics have been evaluated. Rationality of relationships between amount of rainfall and infiltration depth obtained from data analysis has been validated via simulation by using Hydrus-1D. The achieved main conclusions as follows:

(1) Initial soil water content in topsoil and rainfall intensity significantly impact response time of soil water in root zone to rainfall. The lower soil water content in topsoil and the higher rainfall intensity generally cause the shorter response time of soil moisture in root zone (depth of 10 cm) to rainfall.

(2) Generally, infiltration depth increases with increasing of amount of rainfall; infiltration depth of light rain is mostly less than 15 cm, infiltration depth of moderate rain is mostly less than 30 cm, while mostly more than 30 cm for heavy rain and exceeds 60 cm for rainstorm.

(3) Soil water moisture in root zone provide main part (> 70%) of the soil water consumed by ET.

(4) Hydrus-1D is validated that is applicable to simulation of soil water content at the study area, the infiltration depth for different rainfall events can be accurately estimated by using Hydrus-1D under the condition of lack measured soil water content for the study area.

Acknowledgement

The authors gratefully acknowledge the financial support of the National Natural Science Foundation of China (NSFC: 41271046), the 2018 Young Blue Project" of Yangzhou University, China, and the 2019 Science and Technology Innovation Cultivation Fund of Yangzhou University, China (2019cxj069).

Data Availability Statement

The data used in this study has been obtained through field observation and has not been published, which does not conflict with other academic works. All data used during the study appear in the submitted article.

References

Allen R G, Pereira L S, Raes D, Smith M. (1998). Crop Evapotranspiration: Guidelines for Computing Crop Water

Requirements[M]. *FAO*, *Rome*. pp1-300.

Armson D, Stringer P, Ennos A R. (2013). The effect of street trees and amenity grass on urban surface water runoff in Manchester, UK[J]. *Urban Forestry & Urban Greening*, 12(3): 282–286. doi.10.1016/j.ufug.2013.04.001.

Baek S S, Choi D H, Jung J W, Lee H J, Lee H, Yoon K S, Cho K H. (2015). Optimizing low impact development (LID) for stormwater runoff treatment in urban area, Korea: Experimental and modeling approach[J]. *Water Research*, 2015, 86(1): 122–131. doi.org/10.1016/j.watres.2015.08.038.

Chen W L, Li Z S, Jiao L, Wang C, Gao J Y, Fu B J. (2020). Response of soil moisture to rainfall event in black locust plantations at different stages of restoration in hilly-gully area of the Loess Plateau, China[J]. *Chinese Geographical Science*, 30(3): 427–445. doi.org/10.1007/s11769-020-1121-4.

Djaman K, Sall M, Sow A, Manneh B, Irmak S. (2019). Impact of air temperature and relative humidity measured over rice and grass canopies on Penman-Monteith reference evapotranspiration estimates[J]. *J Irrig Drain Eng*, 145(1): 06018008: 1–8.

Duran J, Rodriguez A, Morse J L, Groffman P M. (2013). Winter climate change effects on soil C and N circles in urban grassland[J]. *Global Change Biology*, 19: 2826–2837. doi. 10.1111/gcb.12238.

Fairouz S, Emna G E, Rachida B. (2020). Impact of rainfall structure and climate change on soil and groundwater salinization[J]. *Climatic Change*, 163:395–413. doi.org/10.1007/s10584-020-02789-0.

Fletcher T D, Andrieu H, Hamel P. (2013). Understanding, management and modelling of urban hydrology and its consequences for receiving waters: a state of the art review[J]. *Advances in Water Resources*, 51(1): 261–279.

Hadi H J, Farah A. (2018). Evaluating atmometer performance for estimating reference evapotranspiration in ventilated and unventilated greenhouses[J]. *J Irrig Drain Eng*, 144(7): 04018014: 1–10.

Huang L, Shao M A. (2019). Advances and perspectives on soil water research in China's Loess Plateau[J]. *Earth-Science Reviews*, 199: No.102962: 1–22. doi.org/10.1016/j.earscirev.2019.102962.

Kimura R, Fan J, Zhang X C, Takayama N, Kamichika M, Matsuoka N. (2005). Evapotranspiration over the grassland field in the Liudaogou Basin of the Loess Plateau, China[J]. *Acta Oecologica*, 29(1): 45–53.

Li H, Yi J, Zhang J, Zhao Y, Si B, Hill LR, Cui L, Liu X. (2015). Modeling of soil water and salt dynamics and its effects on root water uptake in Heihe Arid Wetland, Gansu, China[J]. *Water*, 7:2382–2401.

Liu M X, Wang Q Y, Guo L, Yi J, Lin H, Zhu Q, Fan B, Zhang H L. (2020). Influence of canopy and topographic position on soil moisture response to rainfall in a hilly catchment of Three Gorges Reservoir Area, China[J]. *Journal of Geographical Sciences*, 30(6): 949-968. doi.org/10.1007/s11442-020-1764-1.

Liu W, Feng Q, Deo R C, Yao L, Wei W. (2020). Experimental study on the rainfall-runoff responses of typical Urban surfaces and two green infrastructures using scale-based models[J]. *Environmental Management*, 66(4): 683–693.

doi. 10.1007/s00267-020-01339-9.

Longobardi A, Villani P. (2013). The use of micrometeorological data to identify significant variables in evapotranspiration modeling[J]. *Procedia Environmental Sciences*, 19: 263–274.

Livesley S J, Dougherty B J, Smith A J, Luke D, Wylie L J, Arndt S K. (2010). Soil-atmosphere exchange of carbon dioxide, methane and nitrous oxide in urban garden systems: Impact of irrigation, fertiliser and mulch[J]. *Urban Ecosystems*, 13(3): 273–293.

Narjary B, Kumar S, Meena M D, Kamra S K, Sharma D K. (2020). Effects of shallow saline groundwater table depth and evaporative flux on soil salinity dynamics using Hydrus-1D[J]. *Agricultural Research*, doi.org/10.1007/s40003-020-00484-1.

Shi D M, Wang W L, Jiang G Y, Peng X D, Yu Y L, Li Y X, Ding W B. (2016). Effects of disturbed landforms on the soil water retention function during urbanization process in the Three Gorges Reservoir Region, China[J]. *Catena*, 144:84–93. doi. 10.1016/j.catena.2016.04.010.

Song Y S, Li F, Wang X K, Xu C Q, Zhang J Y, Liu X S, Zhang H X. (2015). The effects of urban impervious surfaces on eco-physiological characteristics of Ginkgobiloba: A case study from Beijing, China[J]. *Urban Forestry & Urban Greening*, 14(4): 1102–1109. doi. 10.1016/j.ufug.2015.10.008.

Sutanto S J, Wenninger J, Coenders-Gerrits A M J, Uhlenbrook S. (2012). Partitioning of evaporation into transpiration, soil evaporation and interception: a comparison between isotope measurements and a HYDRUS-1D model[J]. *Hydrology & Earth System Sciences*, 16: 2505–2616. doi.10.5194/hess-16-2605-2012.

Wiekenkamp I, Huisman J A, Bogena H R, Lin H S, Vereecken H. (2016). Spatial and temporal occurrence of preferential flow in a forested headwater catchment[J]. *Journal of Hydrology*, 534: 139–149. doi.org/10.1016/j.j hydrol.2015.12.050.

Wu C, Hao Z C, Liu C Y, Liang J P. (2018). Dynamic change regulation and simulation of soil moisture in Wudaogou Region[J]. *Water Resources and Power*, 36(9): 138–142. (in Chinese)

Xiong L, Xu Z F, Wu F Z, Yang W Q, Yin R, Li Z P, Tang S S, Xiong H T. (2014). Soil respiration of two typical urban lawns in Chengdu City during the winter dormancy period[J]. *Chinese Journal of Applied and Environmental Biology*, 20(2): 275–280. (in Chinese)

Xu Z X, Cheng T. (2019). Basic theory for urban water management and sponge city-review on urban hydrology[J]. *Journal of Hydraulic Engineering*, 50(1): 53–61. (in Chinese)

Yang Q H, Chen L H, Zhang F, Zhang C B. (2008). Responses of soil moisture variations to rainfall and vegetation[J]. *Journal of Beijing Forestry University*, 30(S2): 88–94. (in Chinese)

Yang S M, Zhang T, Zhao Q M, Gao X Y, Wang Z W, He T B. (2020). Factors influencing ecosystem respiration in

510 different cultivated grassland ecosystems in Guiyang[J]. *Pratacultural Science*, 37(11): 2211–2222. (in Chinese)

511 Zang W B, Liu S, Huang S F, Li J R, Fu Y C, Sun Y Y, Zheng J W. (2019). Impact of urbanization on hydrological
512 processes under different precipitation scenarios[J]. *Natural Hazards*, 99(3-SI):12–1257. doi. 10.1007/s11069-018-
513 3534-2.

514 Zhang F M, Shen S H. (2007). Spatial distribution and temporal trend of reference crop evapotranspiration in
515 China[J]. *Journal of Nanjing Institute of Meteorology*, 30(5):705–709. (in Chinese)

516 Zhang R X, Zhao X Y, Zhang C C, Li J. (2020). Impact of rapid and intensive land use/land cover change on soil
517 properties in arid regions: a case study of Lanzhou New Area, China[J]. *Sustainability*, 12(21): No. 9226.
518 doi.org/10.3390/su12219226.

519 Zhao Y F, Zou X Q, Cao L G, Yao Y L, Fu G H. (2018). Spatiotemporal variations of potential evapotranspiration
520 and aridity index in relation to influencing factors over Southwest China during 1960–2013[J]. *Theoretical and*
521 *Applied Climatology*, 133: 711–726. doi.10.1007/s00704-017-2216-4

522 Zhou Q, Huang J B, Zhou Y M, Huang Y Z. (2019). Variation characteristics of evapotranspiration and soil moisture
523 in urban grassland: a case study on the regional grassland vegetation in Yangzhou City[J]. *Water Saving Irrigation,*
524 2019(3): 22–26. (in Chinese)